CrossMark

Comparative numerical analysis using reduced-order modeling strategies for nonlinear large-scale systems

Gabriel Dimitriu [a,*], Răzvan Ştefănescu [b], Ionel M. Navon [c]

[a] *University of Medicine and Pharmacy "Grigore T. Popa", Department of Mathematics and Informatics, Str. Universităţii nr. 16, 700115 Iaşi, Romania*

[b] *North Carolina State University, Department of Mathematics, Raleigh, NC 27615, USA*

[c] *The Florida State University, Department of Scientific Computing, Tallahassee, FL 32306, USA*

ARTICLE INFO

ABSTRACT

We perform a comparative analysis using three reduced-order strategies – Missing Point Estimation (MPE) method, Gappy POD method, and Discrete Empirical Interpolation Method (DEIM) – applied to a biological model describing the spatio-temporal dynamics of a predator–prey community. The comparative study is focused on the efficiency of the reduced-order approximations and the complexity reduction of the nonlinear terms. Different variants are discussed related to the projection-based model reduction framework combined with selective spatial sampling to efficiently perform the online computations. Numerical results are presented.

1. Introduction

The theoretical studies of nonlinear dynamical models pervade the physical, biological, medical and engineering sciences. Nowadays, these investigations are increasingly driven by computational simulations that are of growing complexity and dimension due to increasing computational power and resolution in numerical discretization schemes. In the case of spatio-temporal systems, numerical simulation is typically achieved by spatial discretization of the governing PDEs using, for example, finite volume or finite element methods. The spatial discretization procedure leads to large-scale systems of ordinary differential equations (ODEs), typically of order 10^3–10^8, depending on the complexity of the governing equations and the desired level of accuracy [1–3]. The underlying governing equations are generally nonlinear and the model parameters are often functions of state variables (hence time-varying), which adds considerably to the degree of complexity. Thus, for problems of practical interest, the computational effort required to simulate these systems is substantial. Yet most dynamics of interest are known ultimately to be low-dimensional in nature [4], thus contrasting with the high-dimensional nature of scientific computing.

Reduced-order models (ROMs) are of growing significance in various scientific applications and computing as they help to reduce the computational complexity and time needed to solve large-scale systems. Specifically, ROMs provide a principled approach to approximating high-dimensional spatio-temporal systems.

Although a variety of dimensionality-reduction techniques exist, the ROM methodology is generally based upon the proper orthogonal decomposition (POD) [5,6]. The POD method is ubiquitous in the dimensionality reduction of physical systems. It is alternatively referred to as principal components analysis (PCA) [7], the Karhunen–Loève (KL) decomposition,

* Corresponding author.
   E-mail addresses: dimitriu.gabriel@gmail.com (G. Dimitriu), rstefan@ncsu.edu (R. Ştefănescu), inavon@fsu.edu (I.M. Navon).

empirical orthogonal functions (EOFs) [8], or the Hotelling transform [9]. Snapshots (measurements) of many nonlinear dynamical systems often exhibit low-dimensional phenomena [4], so that the majority of variance and energy is contained in a few modes computed from a singular value decomposition (SVD). For such a case, the POD basis is typically truncated at a predetermined cutoff value, such as when the modal basis contains 99% of the variance only the first r modes (r-rank truncation) are kept. There are numerous additional criteria for the truncation cutoff, and recent results derive a hard-threshold value for truncation that is optimal for systems with well-characterized noise [10]. The SVD acts as a filter, and often the truncated modes correspond to random fluctuations and disturbances. Recently, it has also been proved that it is possible to obtain a *sketched* SVD by randomly projecting the data initially, and then computing the SVD [11,12].

The application of POD is primarily limited to flows whose coherent structures can be hierarchically ranked in terms of their energy content. However, there are situations when the energy content is not a sufficient criterion to accurately describe the dynamical behavior of the aforementioned flows. Instead, the Dynamic Mode Decomposition (DMD) method introduced in [13] links the dominant flow features by a representation in the amplitudes-temporal dominant frequencies space. An improved algorithm for selecting the dominant DMD modes from the flow field is proposed in [14].

Efficiently managing the computation of the nonlinearity (inner products) in dimensionality reduction schemes is of great importance. This was recognized early on in the reduced order modeling community, and a variety of techniques were proposed to accomplish the task. The technique of Everson and Sirovich developed for Gappy data in [15] was among the first methods used in this respect. In their proposed sparse sampling scheme, random measurements were used to perform reconstruction tasks of inner products. Willcox [16] and Karniadakis [17] built on these ideas by advocating principled approaches for selecting sampling locations for Gappy POD. From a mathematical perspective, this technique employs a least-squares regression in one discrete variable using empirical basis functions. Missing Point Estimation (MPE) [18] and Gauss–Newton with approximated tensors (GNAT) [19,20] methods are relying upon the Gappy POD technique to avoid the significant computational cost of nonlinear reduced order models. In the case of GNAT, the nonlinear residual arising at each Newton iteration is approximated by Gappy POD, whereas the fundamental contribution of the MPE method consists in computing Galerkin projections over a restricted subset of the spatial domain.

The Empirical Interpolation Method (EIM) was also developed for the purpose of efficiently managing the computation of the nonlinearity. And as with Gappy POD, principled techniques for sparse measurements where also advocated early on in its history [21]. Whereas Gappy POD applies linear regression, EIM makes use of an interpolation technique to approximate the nonlinear terms. A discrete variant of this technique, the Discrete Empirical Interpolation Method (DEIM), was specifically tailored to POD with Galerkin projection. Indeed, the DEIM approximates the nonlinearity by using a small, discrete sampling of spatial points that are determined using a greedy algorithm. This ensures that the computational cost of evaluating the nonlinearity remains proportional to the rank of the reduced POD basis. As an example, consider the case of an r-mode POD-Galerkin truncation. A simple cubic nonlinearity requires that the POD-Galerkin approximation be cubed, resulting in r^3 operations to evaluate the nonlinear term. The DEIM approximates the cubic nonlinearity by using $\mathcal{O}(r)$ discrete sample points of the nonlinearity, thus preserving the same low-dimensional computation order $\mathcal{O}(r)$, as desired. The DEIM approach combines projection with interpolation. Specifically, the DEIM utilizes selected interpolation indices to specify an interpolation-based projection for a nearly optimal ℓ_2 subspace approximating the nonlinearity. However, they have been successful in a large variety of applications and models [22]. While EIM, DEIM and Gappy POD use a small selected set of spatial grid points to avoid evaluation of the expensive inner products required to evaluate nonlinear terms, the MPE method extends this idea and computes the Galerkin projections over a narrow subset of the spatial domain.

Recently, Sargsyan et al. [23] performed a synthesis of sparse sampling and dimensionality reduction to characterize nonlinear dynamical systems over a range of bifurcation parameters. They constructed modal libraries using the classical proper orthogonal decomposition in order to expose the dominant low-rank coherent structures. To illustrate the new proposed method, the discrete interpolation points and nonlinear modal libraries were used for sparse representation in order to reconstruct the dynamic bifurcation regimes in the complex Ginzburg–Landau equation.

To the best of our knowledge, few results concerning a comparative framework of these three sparsity driven approximations can be found, related to the numerical performance (CPU time, relative errors) with respect to the number of missing/interpolation points involved in these methods. We propose in this paper an interesting comparative study addressing the performance of reduced-order prey–predator models. We are particularly interested in their accuracy and computational costs. Starting point is a conventional POD decomposition from snapshots applied to the solution of a predator–prey biological model incorporating quadratic and cubic nonlinearities. Three sparsity driven approximations are investigated: DEIM, Gappy POD and MPE. The investigation gives conclusive recommendations for the comparative performance of these methods in dependency of the parameters.

The paper is organized as follows. The methods of reduced-order modeling are described in Section 2. Section 2.1 is devoted to Proper Orthogonal Decomposition (POD) method. Section 2.2 is focused on reduced order strategies for nonlinear term approximation by presenting Gappy POD method and Discrete Empirical Interpolation Method (DEIM). Section 2.3 presents Missing Point Estimation (MPE) method. The numerical comparative biological study focused on the efficiency of the reduced-order approximations and the complexity reduction of the reduced order models is analyzed in Section 3. There are described different variants of the projection-based model reduction framework, combined with selective spatial sampling to efficiently perform the online computations. Results of extensive numerical experiments are presented, while conclusions are drawn in Section 4.

2. Reduced order modeling

For high dimensional problems, reduced order modeling is a powerful tool for representing the dynamics of large-scale dynamical systems using only a smaller number of variables and reduced order basis functions. Three approaches will be considered in this study, i.e. Gappy Proper Orthogonal Decomposition (Gappy POD), Discrete Empirical Interpolation Method (DEIM) and Missing Point Estimation (MPE) method to decrease the computational complexity of Proper Orthogonal Decomposition (POD) models due to their inefficiencies when approximating the nonlinear terms.

2.1. Proper Orthogonal Decomposition

Proper Orthogonal Decomposition (POD) has been used successfully in numerous applications such as computational fluid dynamics [24–28], data assimilation [29–31], optimal control and feedback controllers [32–38], oscillating biological networks [39], and together with DEIM in predator–prey models [40], multi-species host–parasitoid systems [41] etc. It can be thought of as a Galerkin approximation in the spatial variable built from functions corresponding to the solution of the physical system at specified time instances.

In what follows, we will only work with discrete inner products (Euclidean dot product) though continuous products may be employed too. Generally, a high-dimensional system of nonlinear partial differential equations is usually governed by the following semi-discrete dynamical system

$$\frac{d\mathbf{y}(t)}{dt} = \mathbf{L}\mathbf{y}(t) + \mathbf{N}(\mathbf{y}(t)), \quad \mathbf{y}(0) = \mathbf{y}_0 \in \mathbb{R}^n, \tag{2.1}$$

where $\mathbf{L}$ and $\mathbf{N}$ are discrete linear and nonlinear operators. From the temporal–spatial flow $\mathbf{y}(t) \in \mathbb{R}^n$, we select an ensemble of N_t time instances $\mathbf{y}_1, \ldots, \mathbf{y}_{N_t} \in \mathbb{R}^n$, n being the total number of discrete model variables per time step and $N_t \in \mathbb{N}$. The method of POD consists in choosing an orthonormal basis $V = \{\mathbf{v}^i\}$, $i = 1, \ldots, k$; $\mathbf{v}^i \in \mathbb{R}^n$; $V \in \mathbb{R}^{n \times k}$ such that the mean square error between $\mathbf{y}(t)$ and POD expansion $\mathbf{y}^{POD}(t) = \bar{\mathbf{y}} + V\tilde{\mathbf{y}}(t), \tilde{y}(t) \in \mathbb{R}^k$ is minimized on average. The mean $\bar{\mathbf{y}} = \frac{1}{N_t} \sum_{i=1}^{N_t} \mathbf{y}_i$ is known as the centering trajectory, shift mode, or mean field correction [36]. Simplified POD expansions do not use the mean in their formulations. For this study we followed a simplified POD expansion $\mathbf{y}^{POD}(t) = V\tilde{\mathbf{y}}(t)$.

The POD basis could be constructed using either the method of snapshots [42–44] or the singular value decomposition method. The latter approach is less affected by numerical errors than the eigenvalue decomposition employed by the method of snapshots. The dimension of the reduced subspace spanned by the $k \ll n$ modes is appropriately chosen to capture the dynamics of the high-fidelity model based on an energy criterion [45, Algorithm 1, step 5].

To obtain the POD reduced order model of (2.1), we first employ a numerical scheme to solve the full model for a set of snapshots and construct the reduced order basis. By applying a Galerkin projection of the full model equations onto the space spanned by the POD basis elements, we obtain the corresponding reduced order model

$$\frac{d\tilde{\mathbf{y}}(t)}{dt} = \tilde{\mathbf{L}}\tilde{\mathbf{y}}(t) + \tilde{\mathbf{N}}(\tilde{\mathbf{y}}(t)), \quad \tilde{\mathbf{y}}(0) = V^T\mathbf{y}(0), \ \tilde{\mathbf{y}}(t) \in \mathbb{R}^k, \quad \text{where}$$
$$\tilde{\mathbf{N}}(\tilde{\mathbf{y}}(t)) = \underbrace{V^T}_{k \times n} \underbrace{\mathbf{N}(V\tilde{\mathbf{y}}(t))}_{n \times 1}. \tag{2.2}$$

Here $\tilde{\mathbf{L}} = V^T\mathbf{L}V$ and we make use of the Euclidean discrete inner product

$$(\mathbf{v}, \mathbf{w})_n = \sum_{\ell=1}^n v_\ell w_\ell, \quad \mathbf{v}, \mathbf{w} \in \mathbb{R}^n \tag{2.3}$$

on the full space $\mathbb{R}^n$ and the orthogonality of the basis modes.

The efficiency of the POD-Galerkin techniques is limited to linear or bilinear terms, since the projected nonlinear term $\tilde{\mathbf{N}}(\tilde{\mathbf{y}}(t)) = V^T\mathbf{N}(V\tilde{\mathbf{y}}(t))$, at every discrete time step, still depends on the number of variables of the full model.

To mitigate this inefficiency, we will employ Gappy POD and DEIM to efficiently approximate the nonlinear reduced order terms. To do so, additional snapshots corresponding to the nonlinear term trajectory will be required for the construction of the nonlinear term reduced basis. This is not the path explored by the MPE method, the additional technique utilized in the present study to decrease the computational complexity of the POD model. While exploring similar ideas as Gappy POD, MPE does not require the construction of an additional basis for the nonlinear terms, since it computes Galerkin projections over a restricted subset of the spatial domain. As such, MPE method can be seen as a collocation method.

2.2. Reduced order strategies for nonlinear term approximation

2.2.1. Gappy POD method

Initially, it was developed in [15] to reconstruct missing or "gappy" data from an available basis. Later on, it was utilized for flow sensing and estimation [16], nonlinear model reduction [20], and approximation of reduced order nonlinear terms [46]. The Gappy POD approximation of the nonlinear term $\mathbf{N}(\mathbf{y}(t)) \in \mathbb{R}^n$ starts from an existing reduced

order basis $U \in \mathbb{R}^{n \times m}$. It can be constructed via POD algorithm from the high-fidelity nonlinear snapshots $\mathbf{N}(\mathbf{y}(t_1))$, $\mathbf{N}(\mathbf{y}(t_2))$, ..., $\mathbf{N}(\mathbf{y}(t_{N_t}))$. Let $J = \{j_1, j_2, \ldots, j_s\} \subset \{1, 2, \ldots, n\}$ be a subset of indices with corresponding mask matrix $P = [\mathbf{e}_{j_1}, \mathbf{e}_{j_2}, \ldots, \mathbf{e}_{j_s}] \in \mathbb{R}^{n \times s}$, where $\mathbf{e}_{j_\ell}$ is the canonical vector with 1 being placed on j_ℓ position.

The most accurate approximation to $\mathbf{N}(\mathbf{y}(t))$ inside the POD manifold U is the orthogonal projection $UU^T\mathbf{N}(\mathbf{y}(t))$ which corresponds to the solution of the least-squares problem

$$\min_{\boldsymbol{\beta} \in \mathbb{R}^m} \|\mathbf{N}(\mathbf{y}(t)) - U\boldsymbol{\beta}\|^2. \tag{2.4}$$

By designing an approximation of $\mathbf{N}(\mathbf{y}(t))$ relying on the information at the indices $j_1, j_2, \ldots, j_s$ and POD basis U, one could construct efficient approximation for reduced order nonlinear term $\tilde{\mathbf{N}}(\tilde{\mathbf{y}}(t))$. This is obtained by solving the masked least-squares problem

$$\min_{\boldsymbol{\beta} \in \mathbb{R}^m} \|P^T\mathbf{N}(\mathbf{y}(t)) - P^TU\boldsymbol{\beta}\|^2. \tag{2.5}$$

This problem is well-defined when P^TU has rank m, thus the number of mask indices s has to be larger or equal to the number of POD modes m. The solution of (2.5) provides an approximation to the nonlinear term $\mathbf{N}(\mathbf{y}(t))$, i.e.

$$\mathbf{N}(\mathbf{y}(t)) \approx U(U^TPP^TU)^{-1}U^TPP^T\mathbf{N}(\mathbf{y}(t)). \tag{2.6}$$

The error between the orthogonal projection $UU^T\mathbf{N}(\mathbf{y}(t))$ and Gappy POD approximation (2.6) is bounded by

$$\|UU^T\mathbf{N}(\mathbf{y}(t)) - U(U^TPP^TU)^{-1}U^TPP^T\mathbf{N}(\mathbf{y}(t))\| \le \|U(U^TPP^TU)^{-1}U^TPP^T\| \|\mathbf{N}(\mathbf{y}(t)) - UU^T\mathbf{N}(\mathbf{y}(t))\| \tag{2.7}$$

according to [46]. Since

$$\|U(U^TPP^TU)^{-1}U^TPP^T\| = \frac{1}{\sigma_{\min}(P^TU)}, \tag{2.8}$$

where $\sigma_{\min}$ denotes the smallest singular value of P^TU, Algorithm 2.1 in [46] provides a way to recursively select the mask indices.

Finally, the Gappy POD reduced nonlinear term approximation of $\tilde{\mathbf{N}}(\tilde{\mathbf{y}}(t))$ is

$$\tilde{\mathbf{N}}(\tilde{\mathbf{y}}(t)) = \underbrace{V^TU(U^TPP^TU)^{-1}U^TP}_{k \times s} \underbrace{P^T\mathbf{N}(V\tilde{\mathbf{y}}(t))}_{s \times 1}, \tag{2.9}$$

which reduces the complexity of the POD nonlinear term since $s \ll n$.

2.2.2. Discrete Empirical Interpolation Method — DEIM

This is a discrete variation of the Empirical Interpolation Method (EIM) proposed by Barrault et al. [47] which provides an efficient technique to approximate nonlinear and non-affine vector-valued functions. The application was suggested and analyzed by Chaturantabut and Sorensen in [48,22,49].

The DEIM approximation of order m for $\mathbf{N}(\mathbf{y}(t))$ in the space spanned by $U \in \mathbb{R}^{n \times m}$ is given by

$$\mathbf{N}(\mathbf{y}(t)) \approx U\mathbf{c}(t), \quad U \in \mathbb{R}^{n \times m}, \ \mathbf{c}(t) \in \mathbb{R}^m. \tag{2.10}$$

The basis U can be constructed effectively by applying the proper orthogonal decomposition (POD) method on some snapshots of the nonlinear term. Next, instead of regression employed by Gappy POD, interpolation is used to determine the coefficient vector $\mathbf{c}(t)$ by selecting m rows $\varrho_1, \ldots, \varrho_m$, $\varrho_i \in \mathbb{N}^*$, of the overdetermined linear system (2.10) to form a m-by-m linear system $P^TU\mathbf{c}(t) = P^T\mathbf{N}(\mathbf{y}(t))$, where $P = [\mathbf{e}_{\varrho_1}, \ldots, \mathbf{e}_{\varrho_m}] \in \mathbb{R}^{n \times m}$, $\mathbf{e}_{\varrho_i} = [0, \ldots, 0, \underbrace{1}_{\varrho_i}, 0, \ldots, 0]^T \in \mathbb{R}^n$.

The DEIM approximation of $\mathbf{N}(\mathbf{y}(t)) \in \mathbb{R}^n$ becomes

$$\mathbf{N}(\mathbf{y}(t)) \approx \underbrace{U(P^TU)^{-1}}_{n \times m} \underbrace{P^T\mathbf{N}(\mathbf{y}(t))}_{m \times 1}. \tag{2.11}$$

Now the only unknowns that need to be specified are the indices $\varrho_1, \varrho_2, \ldots, \varrho_m$ or the matrix P whose dimensions are $n \times m$. This set of indices are inductively constructed from the input POD basis $U = \{\mathbf{u}_\ell\}_{\ell=1}^m \subset \mathbb{R}^n$ by the following greedy algorithm:

ALGORITHM DEIM:
INPUT: $\{\mathbf{u}\}_{\ell=1}^m \subset \mathbb{R}^n$ linearly independent
OUTPUT: $\vec{\varrho} = [\varrho_1, \ldots, \varrho_m]^T \in \mathbb{R}^m$

1. $[|\vec{\varrho}| \ \varrho_1] = \max\{|\mathbf{u}_1|\}$
2. $\mathbf{U} = [\mathbf{u}_1]$, $\mathbf{P} = [\mathbf{e}_{\varrho_1}]$, $\vec{\varrho} = [\varrho_1]$

3. **for** $\ell = 2$ to m **do**
4.   Solve $(\mathbf{P}^T\mathbf{U})\mathbf{c} = \mathbf{P}^T\mathbf{u}_\ell$ for $\mathbf{c}$
5. $\mathbf{r} = \mathbf{u}_\ell - \mathbf{Uc}$
6. $[|\vec{\varrho}|\varrho_\ell] = \max\{|\mathbf{r}|\}$
7. $\mathbf{U} \leftarrow [\mathbf{U}\ \mathbf{u}_\ell],\ \mathbf{P} \leftarrow [\mathbf{P}\ \mathbf{e}_{\varrho_\ell}],\ \vec{\varrho} \leftarrow \begin{bmatrix}\vec{\varrho}\\\varrho_\ell\end{bmatrix}$
8. **end for**

The algorithm is justified by the error bound in [22, Lemma 3.2] depending on the condition number of $(P^TU)^{-1}$. Initially, the algorithm searches for the largest value of the first POD basis $|\mathbf{u}_1|$ and the corresponding index represents the first DEIM interpolation index $\varrho_1 \in \{1, 2, \ldots, m\}$. The remaining interpolation indices $\varrho_\ell, \ell = 2, 3, \ldots, m$ are selected so that each of them corresponds to the entry of the largest magnitude of $|\mathbf{r}|$. The vector $\mathbf{r}$ can be viewed as the residual or the error between the input basis $\mathbf{u}_\ell, \ell = 2, 3, \ldots, m$ and its approximation $\mathbf{Uc}$ from interpolating the basis $\{\mathbf{u}_1, \mathbf{u}_2, \ldots, \mathbf{u}_{\ell-1}\}$ at the indices $\varrho_1, \varrho_2, \ldots, \varrho_{\ell-1}$. The linear independence of the input basis $\{\mathbf{u}_\ell\}_{\ell=1}^m$ guarantees that, in each iteration, $\mathbf{r}$ is a nonzero vector and the output indices $\{\varrho_i\}_{i=1}^m$ are not repeating.

2.3. Missing Point Estimation Method

This approach relies upon Gappy POD developed by [15]. Under suitable conditions we are able to find a finite subset of m distinct points such that

$$\big(\mathbf{v}, \mathbf{w}\big)_n = \big(\mathbf{v}, \mathbf{w}\big)_m, \tag{2.12}$$

where the right inner product is defined in (2.13) and the left product is described in (2.3). By employing the masked product $(\cdot, \cdot)_m$ for the Galerkin projection of the high-fidelity model (2.1), the computational complexity of the obtained reduced order model is much reduced in comparison with the POD model.

For $\mathbf{v}, \mathbf{w} \in \mathbb{R}^n$ let us introduce the bilinear form:

$$\big(\mathbf{v}, \mathbf{w}\big)_m = \sum_{i,j=i_1}^{i_m} v(x_i)q_{ij}w(x_j), \tag{2.13}$$

where q_{ij} is the (i, j) entry of the $m \times m$ real symmetric matrix

$$Q = \tilde{V}\big(\tilde{V}^T\tilde{V}\big)^{-1}\big(\tilde{V}^T\tilde{V}\big)^{-1}\tilde{V}^T, \tag{2.14}$$

and $\tilde{V}$ is defined as

$$\tilde{V} = \begin{pmatrix} v_1(x_{i_1}) & \cdots & v_n(x_{i_1}) \\ v_1(x_{i_2}) & \cdots & v_n(x_{i_2}) \\ \cdots & \cdots & \cdots \\ v_1(x_{i_m}) & \cdots & v_n(x_{i_m}) \end{pmatrix}.$$

Here $V = \{\mathbf{v}^1, \mathbf{v}^2, \ldots, \mathbf{v}^k\}$ is the POD basis of the solution $\mathbf{y}(t)$ defined in Section 2.1, with $v_i(x_{i_1})$ being the i_1 component of POD mode $\mathbf{v}^i$. Moreover, we can write as in the previous section that $\tilde{V} = P^TV$, where P is the proper mask matrix.

According to Lemma 3 in [50], if P^TV is injective, then the equality (2.12) is satisfied for all $\mathbf{v}, \mathbf{w} \in span\{\mathbf{v}^1, \mathbf{v}^2, \ldots, \mathbf{v}^k\}$ and the solution of the reduced order model

$$\frac{d\tilde{\mathbf{y}}(t)}{dt} = \underbrace{V^TPQP^TLV}_{k\times k}\tilde{\mathbf{y}}(t) + \underbrace{V^TPQ}_{k\times m}\underbrace{P^T\mathbf{N}\big(V\tilde{\mathbf{y}}(t)\big)}_{m\times 1}, \quad \tilde{\mathbf{y}}(0) = V^T\mathbf{y}(0),\ \tilde{\mathbf{y}}(t) \in \mathbb{R}^k \tag{2.15}$$

is the solution of the POD model (2.2).

This is the so-called *Missing Point Estimation (MPE) model*. Of course, there are many cases where $\mathbf{w} \notin span\{\mathbf{v}^1, \mathbf{v}^2, \ldots, \mathbf{v}^k\}$ such as $\mathbf{w} = \mathbf{N}\big(V\mathbf{y}(t)\big)$. In this case, there is an alias error introduced by the masked projection depending on the condition number of matrix $(P^TV)^TP^TV - I$. This justifies the use of the following algorithm to select the points $\{x_{i_1}, x_{i_2}, \ldots, x_{i_m}\}$, where we denote by $c(A)$ the condition number of the square matrix A.

ALGORITHM MPE:
INPUT: A (possible empty) set $\mathbf{X}_0^0 \subset \mathbf{X}$ of N_0 pre-selected points, a threshold $c_{tol} > 0$ for the condition number, and a set $\mathbf{Y} \subseteq \mathbf{X}$ of K_0 candidates. Set $j = 0$.
While $c\left(\tilde{V}^T(\mathbf{X}_g)\tilde{V}(\mathbf{X}_g)\right) \leq c_{tol}$ OR $j = K_0$ **do**
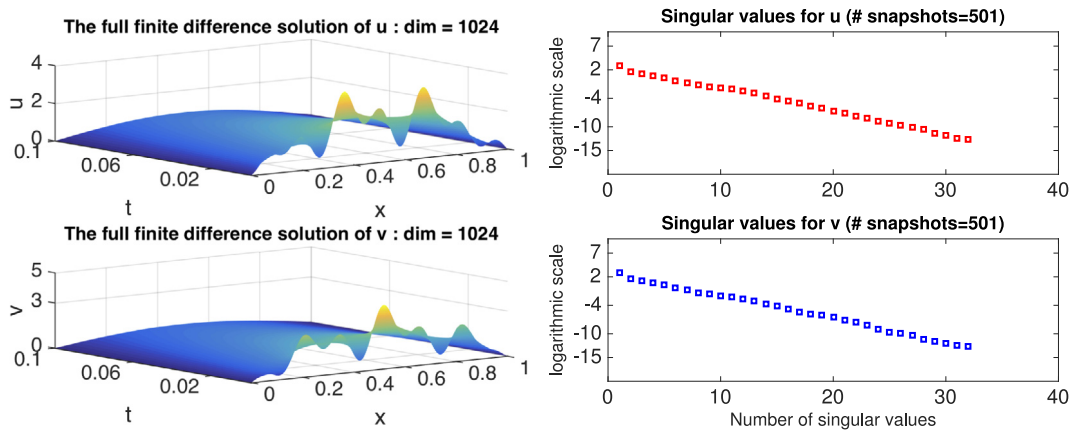
1. Set $j = j + 1$

Fig. 1. Numerical solution of the full-order diffusive predator–prey system with 1024 space points (left plot), and the decreasing of the singular values corresponding to the states u and v (right plot).

2. For all $x_{k_g} \in \mathbf{Y} \setminus \mathbf{X}_0^{j-1}$, determine $c_g = c\left(\tilde{V}^T(\mathbf{X}_g)\tilde{V}(\mathbf{X}_g)\right)$,

   where $\mathbf{X}_g = \mathbf{X}_0^{j-1} \cup \{x_{k_{g*}}\}$ and $g = 1, \ldots, K_0 - j + 1$.
3. Find the index g^* for which $c_{g*} \leq c_g$ for all $1 \leq g \leq K_0 - j + 1$.
4. Set $\mathbf{X}_0^j = \mathbf{X}_0^{j-1} \cup \{x_{k_{g*}}\}$. Then $\mathbf{X}_0^j$ consists of $N_0 + j$ points.

OUTPUT: $\mathbf{X}_0 = \mathbf{X}_0^j$ is a set of $N = N_0 + j$ sample points.

3. Computational issues

This section is devoted to the numerical implementation and a comparative analysis of the reduced-order methods previously described to a predator–prey biological model. The dynamics of a predator–prey system [51], where the prey *per capita* growth rate is damped by the Allee effect [52,53,40,54–56], can be described with nondimensional variables and parameters by the equations with quadratic and cubic nonlinearities:

$$\begin{cases} u_t = u_{xx} - \beta u + (\beta + 1)u^2 - u^3 - uv, \\ v_t = v_{xx} + kuv - mv - \delta v^3, \end{cases} \tag{3.1}$$

where β, k, m and δ are positive dimensionless parameters (fixed at values which ensure the stability of the steady state (u, v)), and subscripts x and t stand for the partial derivatives with respect to dimensionless space and time, respectively. The model is analyzed in [56] and generates predictions in good agreement with the results of qualitative analysis by Owen et al. [57] and with field observations by Fagan et al. [58], both indicating that the biological invasion can be stopped or reversed owing to predation.

Here, we consider the system (3.1) in a bounded domain $\Omega = [0, 1]$ with homogeneous Dirichlet boundary conditions. The initial conditions are given by $u(x, 0) = u_0(x)$ and $v(x, 0) = v_0(x)$, where $u_0(x) = 10x(1 - x)(1 + 0.8 \sin(30x) \cos(10x))$, $v_0(x) = 10x(1 - x)(1 + 0.8 \sin(10x) \cos(30x))$. The densities of the species present initially large fluctuations along the whole space domain, being damped very fast by the Allee effect. The strong Allee effect for prey leads to a very rich dynamics [56] with traveling fronts of invasive species and sensitive to parameter variations [56,59]. The system dynamics (3.1) being strongly damped by the Allee effect, we have chosen a very tight time domain, $[0, T] = [0, 0.1]$. All the numerical simulations were performed using Matlab R2012a [60].

The state system (3.1) was solved numerically using a finite difference discretization. Let $0 = x_0 < x_1 < \cdots < x_n < x_{n+1} = 1$ be equally spaced points on the x-axis for generating the grid points on the dimensionless domain $\Omega = [0, 1]$. The corresponding spatial finite difference discretized system of (3.1) becomes a system of nonlinear ODEs. A first-order integrator (the semi-implicit Euler scheme) was used to solve the discretized system of full dimension, as well as POD–DEIM, Gappy POD and MPE reduced order systems. The numerical scheme is first order in time and second order in space.

Fig. 1 depicts the numerical solution of the full-order diffusive predator–prey system using $n = 1024$ internal space points and 501 time steps (left plot), and the decreasing of the singular values corresponding to the states u and v (right plot). We followed a decoupled approach and built separate bases using snapshots selected at every time step. Similar decreases of the singular values are noticed for both the prey and predator populations. The dimensions of the POD bases for each variable are taken to be 10, capturing more than 99% of the system energy.
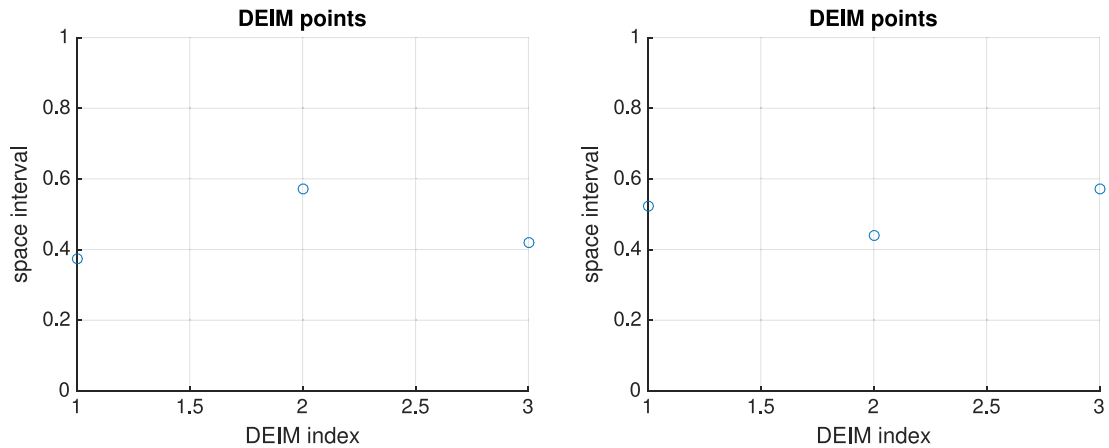
Fig. 2. Distribution of DEIM points for N_1 (left panel) and N_2 (right panel) — dimPOD $= 10$, DEIM $= 3$.

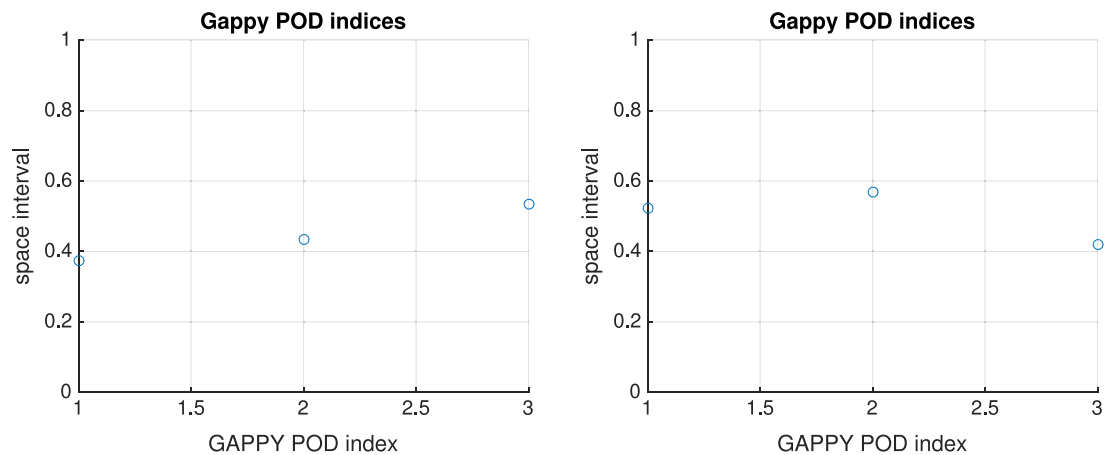**Fig. 3.** Distribution of Gappy indices for N_1 (left panel) and N_2 (right panel) — dimPOD $= 10$, POD $-$ Gappy $= 3$.

We performed numerical simulations with different numbers of DEIM interpolation points, Gappy points and MPE points. We used DEIM and Gappy-POD methods to approximate the nonlinear terms in the model (3.1), i.e.,

$$\begin{cases} N_1 = -\beta u + (\beta + 1)u^2 - u^3 - uv, \\ N_2 = kuv - mv - \delta v^3, \end{cases} \tag{3.2}$$

to decrease the computational cost of the reduced order nonlinearities. Fig. 2 depicts the space locations for a number of 3 DEIM points associated with N_1 (left panel) and N_2 (right panel). The locations of the DEIM points are correlated with the areas where the solutions present the largest fluctuations as seen in Fig. 1.

The locations of the Gappy points depicted in Fig. 3 also target the largest solution variations but differ from those of the DEIM points. Only the first points are identical since both algorithms initially select the largest entry of the first singular vectors. Whereas the DEIM points are used to generate an interpolant, the Gappy points are employed to define a masked regression problem, whose solution is then used to approximate the nonlinear terms. In consequence, the methods apply either interpolation or regression to decrease the computational complexities of the nonlinear reduced order terms.

Whereas the DEIM and Gappy points are associated with the nonlinear terms and their bases, the MPE points define the subset of the spatial domain used by the Galerkin projection and are associated with the POD bases of the solutions. As such, the MPE points are obtained by minimizing the condition number of the matrix $(P^T V)^T P^T V$ described in Algorithm MPE in Section 2.3. The distributions of the MPE points for the first and second equations of the model (3.1) are illustrated in Fig. 4.

Fig. 5 plots the solutions of the reduced-order systems and corresponding relative errors obtained with the POD–DEIM, Gappy-POD and MPE methods. The POD–DEIM and Gappy-POD solutions have similar relative errors while MPE solutions is more accurate. However, it is worth mentioning that the number of MPE points is 30 whereas only 3 DEIM or Gappy points were selected. Experiments with less than 15 MPE points displayed MPE solutions that failed to convergence. Thus we could not use similar number of points for all the methods.

Next, we present the numerical performance of the reduced order models for various number of points; i.e., {1, 2, 3, 5, 10, 15, 20, 40} numbers of DEIM and Gappy points and {15, 20, 30, 50, 100, 200, 300, 400} numbers of MPE points.
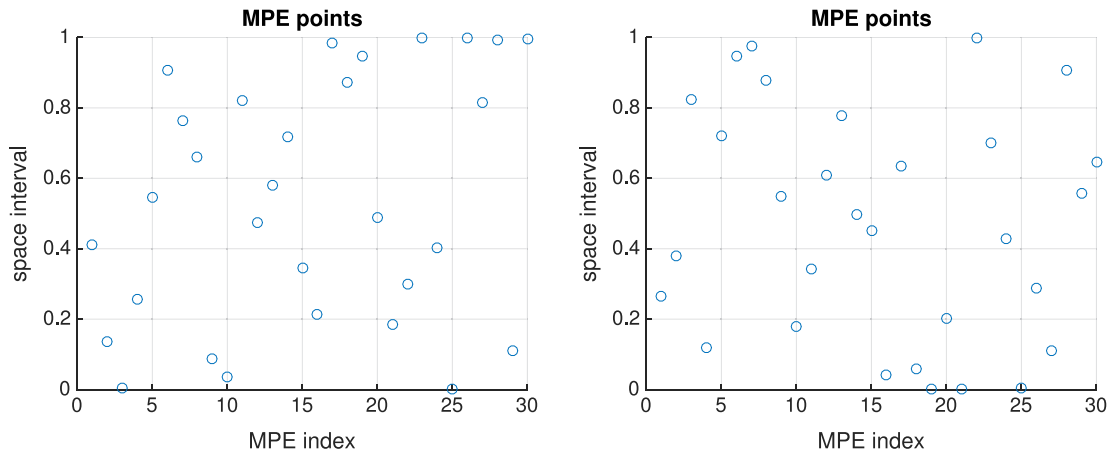
Fig. 4. Distribution of MPE points for the first (left) and the second (right) equation of the model (3.1) − dimPOD = 10, MPE = 30.
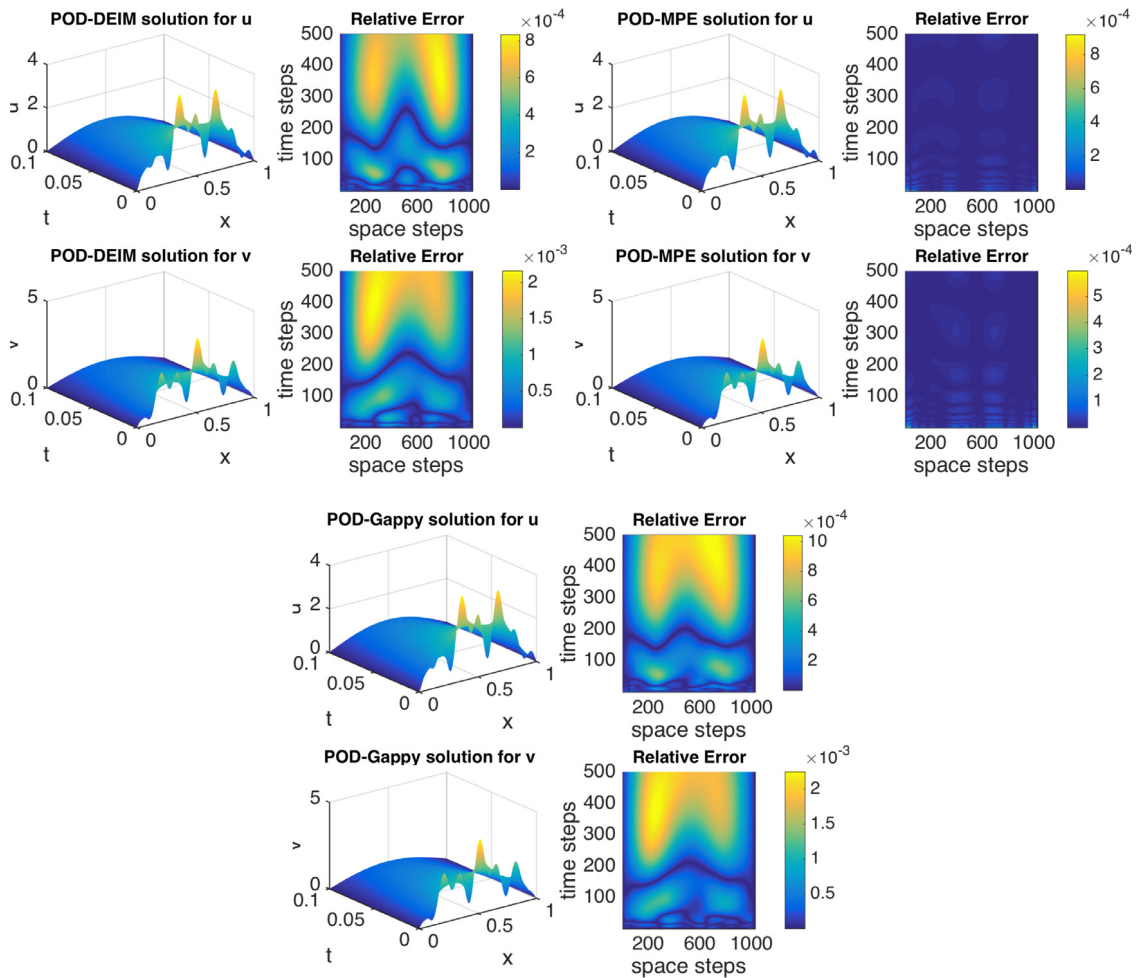

Fig. 5. Plots for the reduced-order numerical approximation of the diffusive predator–prey system using 1024 space points, dimPOD = 10, DEIM = 3, POD − Gappy = 3, and MPE = 30.

Next, we show in Fig. 6 the condition numbers of the matrix $P^T U$ for DEIM and Gappy POD methods, and matrix $(P^T V)^T P^T V$ for MPE method. Here U is the POD basis of a nonlinear term, while V denotes the POD basis of one of the two biological populations. The number of DEIM and Gappy points varies along the lower x-axis, whereas the change in the number of MPE points is represented along the upper x-axis. We notice that the condition numbers of the $(P^T V)^T P^T V$ decrease with
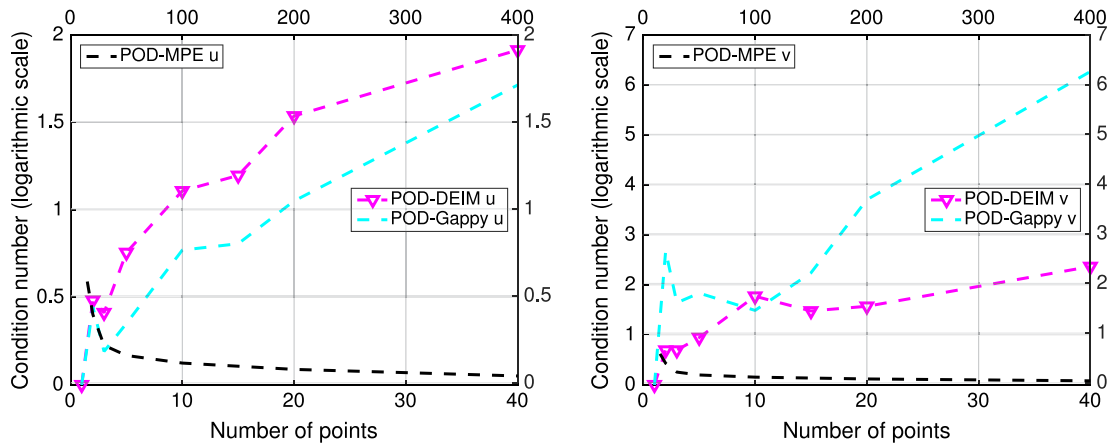
Fig. 6. Condition numbers of the $P^T U$ (DEIM and Gappy POD) and $(P^T V)^T P^T V$ (MPE) for various configuration of points. Here U is generically used to represent the POD basis of either one of the nonlinear terms, while V denotes the POD basis of one of the solutions. The upper x-axis shows the variation in the number of MPE points, while the lower x-axis depicts the change in the number of DEIM or Gappy points.
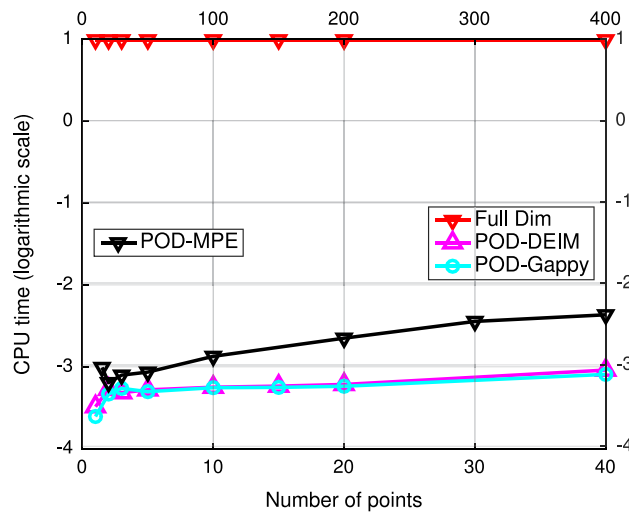

Fig. 7. CPU time for solving the full-order diffusive predator–prey system and reduced-order systems by Gappy POD and POD–DEIM, with respect to the number of interpolation points, and by MPE method varying the number of MPE points. The upper x-axis corresponds to the number of MPE points, while the lower one is associated with the number of DEIM or Gappy POD points.

the increase of the number of MPE points. This is in contrary to the behavior observed for the DEIM and Gappy POD, where the condition numbers increase when using more points.

The on-line computational costs of the high-fidelity and reduced-order models are shown in Table 1. For the same number of points, all the methods have the same computational costs, in accordance with the theoretical expectations. This can be seen by comparing the CPU times for 20 points. The values are given in bold font. For 20 points, all the methods are about 66 times faster than the high-fidelity model.

Even for 400 MPE points, the computational gain is significant, the MPE model being 29 times faster than its full counterpart. This is graphically illustrated in Fig. 7. The reduced order methods have similar computational complexities, with discrepancies caused by the usage of different numbers of points. Again, we remark that MPE solutions failed to converge for less than 15 points explaining the differences in the numbers of points.

The relative errors of the reduced solutions are summarized in Table 2. For 10 points, the POD–DEIM and Gappy POD solutions are accurate with errors of $\mathcal{O}(10^{-4})$ magnitude. All the methods can be compared for 20 points. The results are shown in bold font and we notice a slight decrease in the precision of the MPE solutions.

The relative error results are also graphically depicted in Fig. 8. A very small precision is lost in the case of MPE solutions.

The model reduction techniques Gappy POD, POD–DEIM and MPE method presented in this study have been shown to be efficient for capturing the spatio-temporal dynamics of a diffusive predator–prey model with substantial reduction in both dimension and computational time. This was clearly demonstrated by the comparative computational times shown in Table 1 and by the comparative relative errors of the reduced-order systems with respect to the full-order system shown in

Table 1
CPU time of the full-order system, POD–DEIM, POD–MPE and POD-Gappy using different sets of interpolation points, Gappy points, MPE points, and 1024 internal space points for each variable u and v.

Number of DEIM/Gappy points	MSE points	CPU Time Full Dim	CPU Time POD–DEIM	CPU Time POD–MPE	CPU Time POD-Gappy
1	15	2.699197e+00	3.057996e−02	4.826522e−02	2.712287e−02
2	20	2.699197e+00	3.781034e−02	**4.006125e−02**	3.569973e−02
3	30	2.699197e+00	3.628150e−02	4.391010e−02	3.824401e−02
5	50	2.699197e+00	3.756665e−02	4.557785e−02	3.673999e−02
10	100	2.699197e+00	3.879811e−02	5.531404e−02	3.856367e−02
15	200	2.699197e+00	3.931713e−02	6.912956e−02	3.870378e−02
20	300	2.699197e+00	**4.012907e−02**	8.492089e−02	**3.924228e−02**
40	400	2.699197e+00	4.781416e−02	9.211517e−02	4.536962e−02

Table 2
The relative errors POD–DEIM, POD–MPE and POD-Gappy for u and v using different sets of interpolation points, Gappy points, MPE points, and 1024 internal space points for each variable u and v.

| Number of DEIM/Gappy points	MSE points	Error POD–DEIM – u	Error POD–MPE – u	Error POD-Gappy – u	Error POD–DEIM – v	Error POD–MPE – v	Error POD-Gappy – v
1	15	8.352888e+01	9.927251e−04	8.352888e+01	5.123169e+02	4.820194e−04	5.123169e+02
2	20	1.021814e+00	**2.122344e−04**	1.569596e+00	4.113587e+00	**1.424506e−04**	2.390923e+00
3	30	8.960307e−02	2.156707e−04	1.581963e−01	5.889889e−01	1.303426e−04	6.481559e−01
5	50	5.221578e−04	2.040955e−04	6.690513e−04	5.814482e−04	1.457806e−04	6.092114e−04
10	100	1.345620e−04	1.804276e−04	1.346002e−04	8.412217e−05	1.424006e−04	8.386600e−05
15	200	1.346986e−04	1.712248e−04	1.346782e−04	8.378530e−05	1.212698e−04	8.377125e−05
20	300	**1.346802e−04**	1.607336e−04	**1.346676e−04**	**8.378754e−05**	1.102953e−04	**8.376219e−05**
40	400	1.346687e−04	1.567755e−04	1.346678e−04	8.379207e−05	1.036070e−04	8.379259e−05
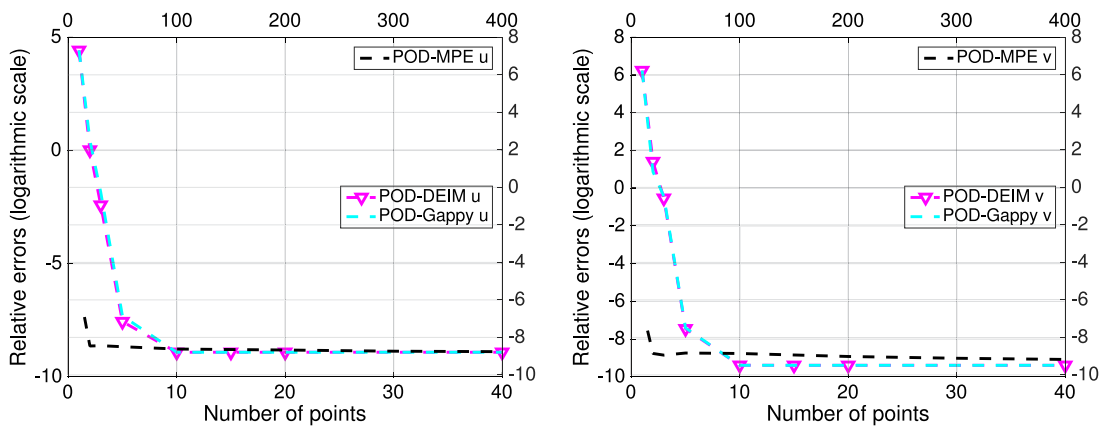
Fig. 8. Relative errors of the solutions to the reduced-order systems with respect to the solution of the full-order system for various numbers of DEIM interpolation points, Gappy-POD indices and MPE points. The upper x-axis shows the variation in the number of MPE points, while the lower x-axis depicts the change in the number of DEIM or Gappy points.

Table 2. The off-line computational complexities of POD–DEIM and Gappy POD methods are higher than those in the case of the MPE model. This is due to the additional SVD factorizations required by the nonlinear term calculations. For small numbers of MPE points, the MPE model failed to converge. For similar numbers of points, all the reduced order models yield similar on-line computational costs. We also notice that Gappy POD and POD–DEIM solutions present similar accuracy levels, whereas MPE solutions suffer a small precision loss.

4. Conclusions

We have performed a comparative study using three reduced-order strategies – Missing Point Estimation (MPE) method, Gappy POD method, and Discrete Empirical Interpolation Method (DEIM) – applied to a biological model describing the spatio-temporal dynamics of a predator–prey community. The comparative analysis was focused on the numerical efficiency and accuracy of the reduced-order approximations and the complexity reduction of the nonlinear terms. We discussed different variants of the projection-based model reduction framework combined with selective spatial sampling to efficiently perform the online computations.

The Gappy POD, POD–DEIM and MPE reduced order biological models constructed in this study have been shown to be accurate and efficient for capturing the spatio-temporal dynamics of a diffusive predator–prey model with substantial reduction in both dimension and computational time. This was clearly demonstrated by the comparative computational times shown in Table 1 and by the comparative relative errors of the reduced-order systems with respect to the full-order system shown in Table 2.

The locations of the DEIM points are correlated with the areas where the solutions present the largest fluctuations. The locations of the Gappy points also target to the largest solution variations, but differ from those of the DEIM points. Only the first points are identical since both algorithms (Gappy POD and DEIM) initially select the largest entry of the first singular vectors. Whereas the DEIM points are used to generate an interpolant, the Gappy points are employed to define a masked regression problem, whose solution is then used to approximate the nonlinear terms. In consequence, the methods apply either interpolation or regression to decrease the computational complexities of the nonlinear reduced order terms.

Comparing the on-line computational costs for both high-fidelity and reduced-order models (see Table 1) we noticed that for the same number of points, all the methods have the same computational costs, in accordance with the theoretical expectations. The off-line computational complexities of POD–DEIM and Gappy POD methods are higher than in the case of the MPE model. This is due to the additional SVD factorizations required by the nonlinear terms calculations. For small numbers of MPE points, the MPE model failed to converge. For similar numbers of points, all the reduced order models have similar on-line computational costs. We also noticed that Gappy POD and POD–DEIM solutions have similar accuracy levels, whereas MPE solutions suffer a small precision loss.

Acknowledgments

References

[1] P. Csomos, R. Cuciureanu, G. Dimitriu, I. Dimov, A. Doroshenko, I. Faragó, K. Georgiev, Á. Havasi, R. Horváth, S. Margenov, Tz. Ostromsky, V. Prusov, D. Syrakov, Z. Zlatev, Impact of Climate Changes on Pollution Levels in Europe, Final report for a NATO Linkage Project (Grant 980505), 2006.
[2] Z. Zlatev, Computer Treatment of Large Air Pollution Models, Kluwer Academic Publishers, Dordrecht, Boston, London, 1995, now distributed by Springer-Verlag, Berlin.
[3] Z. Zlatev, I. Dimov, Computational and Numerical Challenges in Environmental Modelling, Elsevier, Amsterdam, Boston, Heidelberg, London, New York, Oxford, Paris, San Diego, San Francisco, Singapore, Sidney, Tokyo, 2006.
[4] M. Cross, P. Hohenberg, Pattern formation out of equilibrium, Rev. Modern Phys. 65 (1993) 851.
[5] P.J. Holmes, J.L. Lumley, G. Berkooz, C.W. Rowley, Turbulence, Coherent Structures, Dynamical Systems and Symmetry, second ed., in: Cambridge Monographs in Mechanics, Cambridge University Press, Cambridge, England, 2012.
[6] J.L. Lumley, Stochastic Tools in Turbulence, Academic, New York, 1970.
[7] K. Pearson, On lines and planes of closest fit to systems of points in space, Phil. Mag. 2 (1901) 559.
[8] E.N. Lorenz, Empirical orthogonal functions and statistical weather prediction, Technical Report, Massachusetts Institute of Technology (unpublished).
[9] H. Hotelling, Analysis of a complex of statistical variables into principal components, J. Educ. Psychol. 24 (1933) 417.
[10] M. Gavish, D.L. Donoho, The optimal hard threshold for singular values is $4/\sqrt{3}$, IEEE Trans. Inform. Theory 60 (2015) 5040.
[11] J.E. Fowler, Compressive-projection principal component analysis, IEEE Trans. Image Process. 18 (2009) 2230.
[12] H. Qi, S.M. Hughes, Invariance of principal components under low-dimensional random projection of the data, in: IEEE International Conference on Image Processing, IEEE, Orlando, FL, 2012, pp. 937–940.
[13] C.W. Rowley, I. Mezic, S. Bagheri, P. Schlatter, D.S. Henningson, Spectral analysis of nonlinear flows, J. Fluid Mech. 641 (2009) 115–127.
[14] D.A. Bistrian, I.M. Navon, An improved algorithm for the shallow water equations model reduction: Dynamic Mode Decomposition vs POD, Int. J. Numer. Meth. Fluids 78 (2015) 552–580.
[15] R. Everson, L. Sirovich, Karhunen–Loève procedure for gappy data, J. Optim. Soc. Am. A 12 (1995) 1657–1664.
[16] K. Willcox, Unsteady flow sensing and estimation via the gappy proper orthogonal decomposition, Comput. Fluids 35 (2) (2006) 208–226.
[17] B. Yildirim, C. Chryssostomidis, G.E. Karniadakis, Efficient sensor placement for ocean measurements using low dimensional concepts, Ocean Model. 27 (2009) 160.
[18] P. Astrid, Fast reduced order modeling technique for large scale LTV systems, in: Proceedings of the 2004 American Control Conference, vol. 1, IEEE, Boston, MA, 2004, p. 762.
[19] K. Carlberg, C. Farhat, A low-cost, goal-oriented 'compact proper orthogonal decomposition' basis for model reduction of static system, Internat. J. Numer. Methods Engrg. 86 (3) (2011) 381–402.
[20] K. Carlberg, C. Farhat, J. Cortial, D. Amsallem, The GNAT method for nonlinear model reduction: effective implementation and application to computational fluid dynamics and turbulent flows, J. Comput. Phys. 242 (2013) 623–647.
[21] N.C. Nguyen, A.T. Patera, J. Peraire, A "best points" interpolation method for efficient approximation of parametrized functions, Internat. J. Numer. Methods Engrg. 73 (2008) 521.
[22] S. Chaturantabut, D.C. Sorensen, Nonlinear model reduction via discrete empirical interpolation, SIAM J. Sci. Comput. 32 (5) (2010) 2737–2764.
[23] S. Sargsyan, S.L. Brunton, J.N. Kutz, Nonlinear model reduction for dynamical systems using sparse sensor locations from learned libraries, Phys. Rev. E 92 (2015) 033304.
[24] G. Berkooz, P. Holmes, J. Lumley, The proper orthogonal decomposition in the analysis of turbulent flows, Ann. Rev. Fluid Mech. 25 (1993) 777–786.
[25] R. Ştefănescu, I.M. Navon, POD/DEIM nonlinear model order reduction of an ADI implicit shallow water equations model, J. Comput. Phys. 237 (2013) 95–114.
[26] K. Kunisch, S. Volkwein, Galerkin proper orthogonal decomposition methods for a general equation in fluid dynamics, SIAM J. Numer. Anal. 40 (2) (2002) 492–515.
[27] C.W. Rowley, Model reduction for fluids, using balanced proper orthogonal decomposition, Int. J. Bifurcation Chaos 15 (3) (2005) 997–1013.

[28] K. Willcox, J. Peraire, Balanced model reduction via the proper orthogonal decomposition, AIAA J. (2002) 2323–2330.
[29] G. Dimitriu, Using singular value decomposition in conjunction with data assimilation procedures, Lecture Notes in Comput. Sci. 4310 (2007) 435–442.
[30] G. Dimitriu, N. Apreutesei, Comparative study with data assimilation experiments using proper orthogonal decomposition method, Lecture Notes in Comput. Sci. 4818 (2008) 393–400.
[31] G. Dimitriu, N. Apreutesei, R. Ştefănescu, Numerical simulations with data assimilation using an adaptive POD procedure, Lecture Notes in Comput. Sci. 5910 (2010) 165–172.
[32] J.A. Atwell, B.B. King, Proper orthogonal decomposition for reduced basis feedback controllers for parabolic equations. ICAM Report 99-01-01, Virginia Polytechnic Institute and State University, Blacksburg, 1999.
[33] S.L. Brunton, B.R. Noack, Closed-loop turbulence control: progress and challenges, Appl. Mech. Rev. 67 (5) (2015) 050801.
[34] B.R. Noack, K. Afanasiev, M. Morzyński, G. Tadmor, F. Thiele, A hierarchy of low-dimensional models for the transient and post-transient cylinder wake, J. Fluid Mech. 497 (2003) 335–363.
[35] B.R. Noack, M. Morzyński, G. Tadmor (Eds.), Reduced-Order Modelling for Flow Control, in: Series: CISM International Centre for Mechanical Sciences, vol. 528, Springer, 2011.
[36] B.R. Noack, M. Schlegel, M. Morzyński, G. Tadmor, System reduction strategy for Galerkin models of fluid flows, Internat. J. Numer. Methods Fluids 63 (2) (2010) 231–248.
[37] K. Kunisch, S. Volkwein, Control of the Burgers' equation by a reduced order approach using proper orthogonal decomposition, J. Optim. Theory Appl. 102 (2) (1999) 345–371.
[38] W. Stankiewicz, M. Morzyński, R. Roszak, B.R. Noack, G. Tadmor, Reduced order modelling of a flow around an airfoil with a changing angle of attack, Arch. Mech. 60 (6) (2008) 509–526.
[39] A.M. Rehm, E.Y. Scribner, H.M. Fathallah-Shaykh, Proper orthogonal decomposition for parameter estimation in oscillating biological networks, J. Comput. Appl. Math. 258 (2014) 135–150.
[40] G. Dimitriu, I.M. Navon, R. Ştefănescu, Application of POD-DEIM approach for dimension reduction of a diffusive predator–prey system with allee effect, Lecture Notes in Comput. Sci. 8353 (2014) 373–381.
[41] G. Dimitriu, R. Ştefănescu, I.M. Navon, POD-DEIM approach on dimension reduction of a multi-species host-parasitoid system, Ann. Acad. Rom. Sci. Ser. Math. Appl. 7 (1) (2015) 173–188.
[42] L. Sirovich, Turbulence and the dynamics of coherent structures. I. Coherent structures, Quart. Appl. Math. 45 (3) (1987) 561–571.
[43] L. Sirovich, Turbulence and the dynamics of coherent structures. II. Symmetries and transformations, Quart. Appl. Math. 45 (3) (1987) 573–582.
[44] L. Sirovich, Turbulence and the dynamics of coherent structures. III. Dynamics and scaling, Quart. Appl. Math. 45 (3) (1987) 583–590.
[45] R. Ştefănescu, A. Sandu, I.M. Navon, Comparison of POD reduced order strategies for the nonlinear 2D shallow water equations, Internat. J. Numer. Methods Fluids 76 (8) (2014) 497–521.
[46] R. Zimmermann, K. Willcox, An accelerated greedy missing point estimation procedure, SIAM J. Sci. Comput., 2016. Preprint.
[47] M. Barrault, Y. Maday, N.C. Nguyen, A.T. Patera, An "empirical interpolation" method: application to efficient reduced-basis discretization of partial differential equations, C. R. Math. Acad. Sci., Paris 339 (2004) 667–672.
[48] S. Chaturantabut, Dimension Reduction for Unsteady Nonlinear Partial Differential Equations via Empirical Interpolation Methods, Technical Report TR09-38, CAAM, Rice University, 2008.
[49] S. Chaturantabut, D.C. Sorensen, A state space error estimate for POD-DEIM nonlinear model reduction, SIAM J. Numer. Anal. 50 (1) (2012) 46–63.
[50] P. Astrid, S. Weiland, K. Willcox, T. Backx, Missing point estimation in models described by Proper Orthogonal Decomposition, IEEE Trans. Automat. Control 53 (10) (2008) 2237–2251.
[51] J.D. Murray, Mathematical Biology, second ed., Springer, Berlin, 1993.
[52] W.C. Allee, The Social Life of Animals, Norton and Co., New York, 1938.
[53] B. Dennis, Allee effects: population growth, critical density, and the chance of extinction, Nat. Resour. Model. 3 (1989) 481–538.
[54] P. Georgescu, H. Zhang, D. Maxin, The global stability of coexisting equilibria for three models of mutualism, Math. Biosci. Eng. 13 (1) (2016) 101–118.
[55] A.Y. Morozov, S.V. Petrovskii, B.-L. Li, Bifurcations and chaos in a predator–prey system with the Allee effect, Proc. R. Soc. B 271 (2004) 1407–1414.
[56] S.V. Petrovskii, H. Malchow, B.-L. Li, An exact solution of a diffusive predator–prey system, Proc. R. Soc. Lond. Ser. A Math. Phys. Eng. Sci. 461 (2005) 1029–1053.
[57] M.R. Owen, M.A. Lewis, How predation can slow, stop or reverse a prey invasion, Bull. Math. Biol. 63 (2001) 655–684.
[58] W.F. Fagan, J.G. Bishop, Trophic interactions during primary succession: herbivores slow a plant reinvasion at Mount St. Helens, Amer. Nat. 155 (2000) 238–251.
[59] V. Volpert, S. Petrovskii, Reaction–diffusion waves in biology, Phys. Live Rev. 6 (2009) 267–310.
[60] MATLAB, version 7.14.0.739 (R2012a), The MathWorks Inc., Natick, Massachusetts, 2012.